

## Exploring Ion Permeation Energetics in Gramicidin A Using Polarizable Charge Equilibration Force Fields

Sandeep Patel,\* Joseph E. Davis, and Brad A. Bauer

Department of Chemistry and Biochemistry, University of Delaware, Newark, Delaware 19716

Received April 17, 2009; E-mail: sapatel@udel.edu

All-atom molecular dynamics simulations have been applied in the recent past to explore the free energetics underlying ion transport processes in biological ion channels. Roux and co-workers,<sup>1–4</sup> Kuyucak and co-workers,<sup>5</sup> Busath and co-workers,<sup>6</sup> and others have performed rather elegant and extended time scale molecular dynamics simulations using current state-of-the-art fixed-charge (nonpolarizable) force fields to calculate the potential of mean force defining the equilibrium flux of ions through prototypical channels such as gramicidin A. Such studies overestimate the permeation free energy barrier, generally predicting maximum heights from 10 to 20 kcal/mol depending on the force field and simulation protocol used. This translates to an underestimation of experimentally measurable single channel conductances by several orders of magnitude. Next-generation polarizable force fields<sup>7–9</sup> have been suggested as possible alternatives for more quantitative predictions of the underlying free energy surface in such systems.<sup>1</sup> Presently, we consider ion permeation energetics in the gramicidin A channel using a polarizable force field.

We apply a charge equilibration polarizable force field for lipids, water, and protein; the small, hard potassium cation is treated as a nonpolarizable entity. This is a sufficiently justified approximation as the polarizability of potassium<sup>10</sup> is  $0.83 \text{ \AA}^3$ , which is smaller than the polarizability of solvent, lipid, and protein constituents. Moreover, without performing full hydration free energy calculations to assess the ion–water and ion–protein interactions, we computed gas-phase interaction energies for  $\text{K}^+$  with TIP4P-FQ (solvent model employed currently) and the *N*-methylacetamide molecule (an often-used proxy for interactions with a peptide backbone). The current force field combination yields a TIP4P-FQ to ion interaction energy of  $-15.7 \text{ kcal/mol}$  and an NMA to potassium ion interaction energy of  $-28.5 \text{ kcal/mol}$ . The respective *ab initio* values (calculated for this work at the MP2/cc-pVTZ level) are  $-15.65$  and  $-30.02 \text{ kcal/mol}$ , and experimental binding affinity (enthalpy) values are  $-16.2$  and  $-29.83 \text{ kcal/mol}$ , respectively. Thus the current force field captures the *relative driving force* for partitioning between bulk solvent and peptide channel (at least at the level of matching gas-phase binding affinity from experiment and *ab initio* calculations).<sup>11</sup>

Further details of the simulation system and MD protocol are given in the Supporting Information. Structural integrity of the gA channel is monitored via the root-mean-squared deviation from the initial structure, obtained by equilibrating the crystal structure (PDB entry 1JNO).<sup>12</sup> From Figure 1 it is evident that over the course of extended time-scale MD simulations, the structure of the channel is robust for the calculations at hand. Data are shown for simulations with a free gA channel in a DMPC bilayer; similar behavior is observed for the channel structure with a restrained ion. Figure 2 shows the one-dimensional potential of mean force computed using umbrella sampling with post-simulation data processing using the WHAM equations.<sup>13,14</sup> The current polarizable force field shows a dramatic decrease in the central barrier to ion permeation.

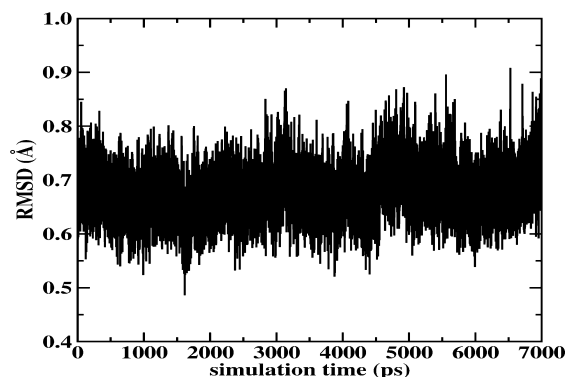


Figure 1. Backbone rmsd for gA embedded in a DMPC bilayer. Rmsd relative to PDBID:1JNO structure.<sup>12</sup>

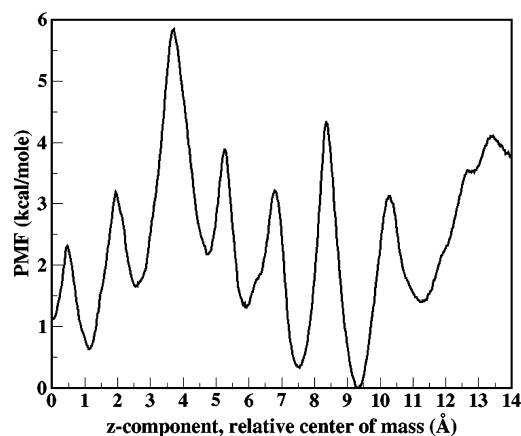
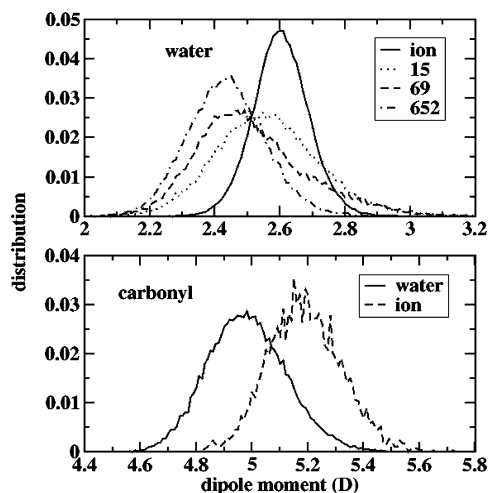


Figure 2. 1-D Potential of Mean Force. The *x*-axis corresponds to the *z*-component of the center of mass separation between the gA dimer and  $\text{K}^+$  ion.

Furthermore, we stress that no corrections to the PMF (for ionic strength and system periodicity) have been included (though the effects of such corrections will no doubt further reduce inherent barriers; such a study is outside the scope of the present communication and is reserved for a future study). Assuming a constant channel  $\text{K}^+$  diffusion coefficient (reduced by one-tenth from the bulk value), we estimate a maximum conductance of 57 pS, in semiquantitative agreement with the experimental value of 24 pS (picoSiemens)<sup>1,3</sup> (Supporting Information). The global minimum occurs at a 9.5 Å relative center of mass separation, in excellent agreement with the solid state  $\text{N}^{15}$  NMR chemical shift anisotropy experiments of Tian et al.<sup>15</sup> Moreover, the site at 7.5 Å is seen to be of low free energy (almost commensurate in stability to the global binding site) but separated by a significant free energy barrier of 5 kcal/mol. This further coincides with the NMR measurements<sup>15</sup> suggesting an internal binding site of significantly reduced signal



**Figure 3.** Water dipole moment distributions (top panel) for water coordinating with ion (solid line) and channel waters coordinating with gA backbone carbonyl groups. The numbers 15, 69, and 652 label channel waters starting at the channel opening and moving to the channel center. Bottom panel shows distributions for backbone carbonyl groups (residue TRP13) coordinating with channel waters (solid line) and restrained channel ion (dashed line).

relative to the external binding sites (conjectured to be of equal free energy). We note that nonpolarizable force fields in general predict similar locations of local minima, but the relative energetics are force field dependent. For the CHARMM nonpolarizable force field, the global minimum is 12.5 Å, while the current polarizable force field shows a global minimum at 9.5 Å.

Since the subtle, local interactions between the ion and coordinating ligands and channel water primarily impact ion translocation within this channel, we consider in Figure 3 dipole moment distributions of ion-coordinating water molecules and backbone carbonyl groups; Figure 3 (top panel) shows the distributions for water molecules only in the channel for the cases where the water is interacting only with backbone carbonyl groups and when the water is also coordinating the ion. Likewise, for the carbonyl groups (Figure 3, bottom panel), we investigate the dipole moment for groups coordinating one water molecule and those coordinating the ion. We also consider specific residues to highlight the residue

dependence (local environmental dependence) of the water and carbonyl electrostatics that is possible to capture with polarization effects. The bottom panel of Figure 3 shows the shift in carbonyl dipole moment between coordination with water (solid curve) and ion (dashed curve). This shift is on the order of 0.2 D, and this in conjunction with the enhanced water dipole moments agrees with the deep free energy minima corresponding to the binding sites along the channel axis. The induced dipole thus provides a compensatory stabilization for the ion being desolvated. This stabilization is lacking in nonpolarizable force fields. Furthermore, the binding site stability is evidenced by the larger barriers presenting as the ion moves out of the binding sites; for the inner binding sites, the polarizable force field PMF shows barriers of 4–5 kcal/mol (i.e., moving toward the inner channel from sites at 9.5, 7.5, and 5 Å).

**Acknowledgment.** The authors acknowledge support from an NIH COBRE (Grant No. P20RR015588) at the Univ. of Delaware, Department of Chemical Engineering.

**Supporting Information Available:** Simulation protocol and information on force fields. This material is available free of charge via the Internet at <http://pubs.acs.org>.

## References

- (1) Allen, T. W.; Andersen, O. S.; Roux, B. *Proc. Natl. Acad. Sci. U.S.A.* **2004**, *101* (1), 117–122.
- (2) Allen, T. W.; Andersen, O. S.; Roux, B. *Biophys. J.* **2006**, *90*, 3447–3468.
- (3) Roux, B.; Allen, T.; Berneche, S.; Im, W. *Q. Rev. Biophys.* **2004**, *37*, 15–103.
- (4) Roux, B.; Karplus, M. *Biophys. J.* **1991**, *59*, 961–981.
- (5) Kuyucak, S.; Andersen, O. S.; Chung, S.-H. *Rep. Prog. Phys.* **2001**, *64*, 1427–1472.
- (6) Busath, D. D. *Annu. Rev. Physiol.* **1993**, *55*, 473–501.
- (7) Davis, J. E.; Rahaman, O.; Patel, S. *Biophys. J.* **2009**, *96* (2), 385–402.
- (8) Davis, J. E.; Warren, G. L.; Patel, S. *J. Phys. Chem. B* **2008**, *112*, 8298.
- (9) Ren, P.; Ponder, J. W. *J. Phys. Chem. B* **2003**, *107*, 5933–5947.
- (10) Mahan, G. D. *Phys. Rev. A* **1980**, *22*, 1780–1785.
- (11) Siu, S. W. I.; Vacha, R.; Jungwirth, P.; Bockmann, R. A. *J. Chem. Phys.* **2008**, *128*, 125103.
- (12) Townsley, L. E.; Tucker, W. A.; Sham, S.; Hinton, J. F. *Biochemistry* **2001**, *40*, 11676–11686.
- (13) Kumar, S.; Bouzida, D.; Swendsen, R. H.; Kollman, P. A.; Rosenberg, J. M. *J. Comput. Chem.* **1992**, *13*, 1011–1021.
- (14) Kumar, S.; Rosenberg, J. M.; Bouzida, D.; Swendsen, R. H.; Kollman, P. A. *J. Comput. Chem.* **1995**, *16*, 1339–1350.
- (15) Tian, F.; Cross, T. A. *J. Mol. Biol.* **1998**, *285* (5), 1993–2003.

JA902903M